

Crystal Structure and Magnetic Properties of a New Chiral Manganese(II) Three-Dimensional Framework: $\text{Na}_3[\text{Mn}_3(\text{HCOO})_9]$

Verónica Paredes-García*

Departamento de Química, Universidad Tecnológica Metropolitana, Chile

Andrés Vega

Facultad de Ecología y Recursos Naturales, Universidad Andres Bello, Chile

Miguel A. Novak

Instituto de Física, Universidade Federal do Rio de Janeiro, Brazil

Maria G. F. Vaz and Denise A. Souza

Instituto de Química, Universidade Federal Fluminense, Brazil

Diego Venegas-Yazigi

Departamento de Química de los Materiales, Universidad de Santiago de Chile, Chile

Evgenia Spodine

Facultad de Ciencias Químicas y Farmacéuticas, Universidad de Chile, Chile

Received October 10, 2008

A structural and magnetic characterization of a trinuclear chiral Mn(II) formate three-dimensional framework exhibiting a triangular arrangement is presented. Compound $\text{Na}_3[\text{Mn}_3(\text{HCOO})_9]$ was obtained by solvothermal synthesis and crystallizes in the chiral cubic space group $P2_13$ and is well described by a Δ conformation. The structure displays triangular Mn_3 building blocks, in which the metal centers are bonded by formate ligands in a *syn-anti* mode (Mn–Mn 5.697(1) Å). The coordination sphere of manganese(II) is completed by six oxygen atoms from six formate ligands, resulting in an octahedral geometry. Magnetic susceptibility measurements showed antiferromagnetic interactions at high temperature and a strongly field dependent magnetic behavior below 40 K. At fields higher than 1.0 kOe only the antiferromagnetic interactions can be observed. At applied fields lower than 1.0 kOe magnetic susceptibility becomes irreversible with maxima observed at 22 and 34 K. These maxima suggest a weak ferromagnetic behavior because of spin canting, allowed by the presence of the noncentrosymmetric *syn-anti* HCOO bridges linking the Mn sites. This non-collinear antiferromagnetism and irreversible behavior can be due to the existence of a high degree of frustration in this unique lattice composed of linked triangular arrangements of interacting magnetic centers.

Introduction

There is currently much interest in creating new materials combining magnetism with other properties such as conductivity, optical properties, or porosity.¹ The rational design of

these new magnetic materials requires taking into account two important aspects: the nature of both the spin carriers

*To whom correspondence should be addressed. E-mail: vpg@manquehue.net.

(1) (a) Sato, O.; Tao, J.; Zhang, Y. Z. *Angew. Chem., Int. Ed.* **2007**, *46*, 2152. (b) Sato, O. *Acc. Chem. Res.* **2003**, *36*, 692. (c) Decurtins, S.; Pellaux, R.; Antorrena, G.; Palacio, F. *Coord. Chem. Rev.* **1999**, *190–192*, 841. (d) Coronado, E.; Day, P. *Chem. Rev.* **2004**, *104*, 5419. (e) Gütlich, P.; Garcia, Y.; Woike, T. *Coord. Chem. Rev.* **2001**, *219–221*, 839. (f) Talham, D. R. *Chem. Rev.* **2004**, *104*, 5479.

and the bridges. Generally, 3d transition metal ions have been considered as the spin carriers, and short conjugated ligands as bridges. Three-atom bridges are particularly interesting in several aspects: (i) they can transfer magnetic interactions, (ii) they have a variety of coordination and bridging modes to transition metal centers, which makes them useful to tailor various interesting structures, and (iii) they may preclude the existence of an inversion center between the two bridged metal ions and therefore allow the antisymmetric interaction (Dzyaloshinsky–Moriya interaction, DM) between the metal centers.²

The use of carboxylate ligands and their derivatives as three-atom bridges has played an important role in the field of materials chemistry, allowing the generation of polynuclear complexes ranging from discrete entities to three-dimensional (3D) systems.³ The formate anion HCOO^- is the smallest and simplest carboxylate and has been extensively employed in creating materials with interesting magnetic properties. Depending on the conformation of the formate bridge (*anti-anti*, *syn-anti*, *syn-syn* among others) this can mediate ferromagnetic or antiferromagnetic coupling.^{4–9}

Divalent 3D metal-formate frameworks such as $\text{M}(\text{HCOO})_2 \cdot 2\text{H}_2\text{O}$ ($\text{M} = \text{Mn, Fe, Co, Ni}$ and Cu)^{5–12} exhibit predominantly long-range antiferromagnetic ordering. $\text{M}(\text{HCOO})_2\text{L}_2$, where L is a coligand such as urea or formamide, shows spontaneous magnetization at the Néel transition because of canting of the moments of the sublattices.^{3b,13}

$[\text{NH}_4][\text{Mn}(\text{HCOO})_3]^{14}$ crystallizes in the hexagonal chiral space group $P6_322$, where the chirality arises from the

handedness imposed by the formate ligands around the metal ions and the presence of units with only one handedness. Chiral magnets (bifunctional materials) are very attractive because of their potential technological applications.¹⁵ Since the chirality of the compounds must be controlled in the molecular structure, as well as in the entire crystal structure, only a few examples of this type of magnets exist.

On the other hand, spin frustration in paramagnetic species is of current interest because of its influence on physical properties.¹⁶ In this type of compounds, the topology of the complex or lattice causes the antiferromagnetic interactions not to be satisfied completely leading to geometrically frustrated magnets (GFMs).¹⁷ The oxo-centered carboxylate complexes $[\text{M}_3\text{O}(\text{O}_2\text{CR})_n\text{L}_m]^{18}$ are the best examples of this magnetic behavior. Therefore, it is of interest to find new synthetic approaches that allow new materials to be obtained with topologies leading to novel multifunctional properties.

In this paper we present the structural and magnetic characterization of a new chiral 3D network based on the trinuclear $\text{Mn}(\text{II})$ formate unit $\text{Na}_3[\text{Mn}_3(\text{HCOO})_9]$, exhibiting a triangular arrangement, as an example of a new material with a crystalline topology in which it is possible to find chirality, spin canting, and spin frustration phenomena.

Experimental Section

All starting materials were commercially available reagents of analytical grade, and were used without further purification. $\text{Na}_3[\text{Mn}_3(\text{HCOO})_9]$ was obtained in 30% yield by solvothermal synthesis in dimethylformamide (DMF) in a 23 mL Teflon-lined stainless steel autoclave at 170 °C for 24 h under self-generated pressure. After slow cooling (0.05 °C/min) to room temperature the solid product was filtered and dried at 40 °C. The reagents were used in a $\text{Mn}(\text{CH}_3\text{COO})_2 \cdot 4\text{H}_2\text{O}$: L-serine/ Na_3PO_4 /DMF molar ratio of 2:1:3:160. X-ray diffraction quality, pale yellow single crystals were directly separated from the bulk material.

Single-Crystal X-ray Diffraction. The crystal structure of $\text{Na}_3[\text{Mn}_3(\text{HCOO})_9]$ (**1**) was determined by X-ray diffraction on a $0.14 \times 0.12 \times 0.12$ mm³ single crystal. Data collection was performed on a Bruker-Kappa-CCD diffractometer, with graphite-monochromatized $\text{Mo K}\alpha$ radiation ($\lambda = 0.71073$ Å) at room temperature. Final unit cell parameters were based on the fitting of all reflection positions (DIRAX9).¹⁹ Data integration and scaling of the reflections were performed with the EVALCCD suite.²⁰ Empirical multiscan absorption corrections using equivalent reflections were performed with the program SADABS.²¹ The structure was solved and refined against F^2 by full-matrix least-squares techniques using the SHELXTL software package.²² Hydrogen atoms were placed in calculated

- (2) Wang, X. Y.; Wang, Z. M.; Gao, S. *Chem. Commun.* **2008**, 281.
 (3) (a) Doedens, R. J. *Prog. Inorg. Chem.* **1976**, *21*, 209. (b) Rettig, S. J.; Thompson, R. C.; Trotter, J.; Xia, S. *Inorg. Chem.* **1999**, *38*, 1360. (c) Tangoulis, V.; Psomas, G.; Dendrinou-Samara, C.; Raptopoulou, C. P.; Terzis, A.; Kessissoglou, D. P. *Inorg. Chem.* **1996**, *35*, 7655. (d) Dey, S. K.; Bag, B.; Malik, K. M. A.; Salah El Fallah, M.; Ribas, J.; Mitra, S. *Inorg. Chem.* **2003**, *42*, 4029. (e) Piñero, D.; Baran, P.; Boca, R.; Herchel, R.; Klein, M.; Raptis, R.; G.; Renz, F.; Sanakis, Y. *Inorg. Chem.* **2007**, *46*, 10981.
 (4) (a) Mehrotra, R. C.; Bhora, R. In *Metal Carboxylates*; Academic Press: New York, 1983. (b) Oldham, C. *Prog. Inorg. Chem.* **1968**, *10*, 223. (c) Carrell, C. J.; Carrell, H. L.; Erlebacher, J.; Glusker, J. P. *J. Am. Chem. Soc.* **1988**, *110*, 8651.
 (5) (a) Osaki, K.; Nakai, Y. *J. Phys. Soc. Jpn.* **1963**, *18*, 919. (b) Osaki, K.; Nakai, Y.; Watanabé, T. *J. Phys. Soc. Jpn.* **1964**, *19*, 717. (c) Abe, H.; Morigaki, H.; Matsuura, M.; Torh, K.; Yamagata, K. *J. Phys. Soc. Jpn.* **1964**, *19*, 775. (d) Abe, H.; Torh, K. *J. Phys. Soc. Jpn.* **1965**, *20*, 183. (e) Yamagata, K.; Abe, H. *J. Phys. Soc. Jpn.* **1965**, *20*, 906. (f) Yamagata, K. *J. Phys. Soc. Jpn.* **1967**, *22*, 582. (g) Pierce, R. D.; Friedberg, S. A. *Phys. Rev.* **1968**, *165*, 680. (h) Takeda, K.; Kawasaki, K. *J. Phys. Soc. Jpn.* **1971**, *31*, 1026. (i) Radhakrishna, P.; Gillon, B.; Chevrier, G. *J. Phys.: Condens. Matter* **1993**, *5*, 6447.
 (6) (a) Hoy, G. R.; Barros, S. de S.; Barros, F. de S.; Friedberg, S. A. *J. Appl. Phys.* **1965**, *36*, 936. (b) Pierce, R. D.; Friedberg, S. A. *Phys. Rev. B* **1971**, *3*, 934.
 (7) Kaufman, A.; Afshar, C.; Rossi, M.; Zacharias, D. E.; Glusker, J. P. *Struct. Chem.* **1993**, *4*, 191.
 (8) Kageyama, H.; Khomskii, D. I.; Levitin, R. Z.; Vasil'ev, A. N. *Phys. Rev. B* **2003**, *67*, 224422.
 (9) (a) Martin, R. L.; Waterman, H. *J. Chem. Soc.* **1959**, 1359. (b) Flippen, R. B.; Friedberg, S. A. *J. Chem. Phys.* **1963**, *38*, 2652. (c) Kobayashi, H.; Haseda, T. *J. Phys. Soc. Jpn.* **1963**, *18*, 541.
 (10) Sapiña, F.; Burgos, M.; Escrivá, E.; Folgado, J.-V.; Marcos, D.; Beltrán, A.; Beltrán, D. *Inorg. Chem.* **1993**, *32*, 4337.
 (11) Viertelhaus, M.; Henke, H.; Anson, C. E.; Powell, A. K. *Eur. J. Inorg. Chem.* **2003**, 2283.
 (12) (a) Wang, Z.-M.; Zhang, B.; Fujiwara, H.; Kobayashi, H.; Kurmoo, M. *Chem. Commun.* **2004**, 416. (b) Dybtsev, D. N.; Chun, H.; Yoon, S. H.; Kim, D.; Kim, K. *J. Am. Chem. Soc.* **2004**, *126*, 32.
 (13) Ridwan, X. *Jpn. J. Appl. Phys.* **1992**, *31*, 3559.
 (14) Wang, Z.; Zhang, B.; Inoue, K.; Fujiwara, H.; Otsuka, T.; Kobayashi, H.; Kurmoo, M. *Inorg. Chem.* **2007**, *46*, 437.

(15) Inoue, K.; Ohkoshi, S. I.; Imai, H. In *Magnetism: Molecules to Materials V*; Miller, J. S., Drillon, M., Eds.; Wiley-VCH Verlag GmbH & Co. KGaA: Weinheim, Germany, 2005; Chapter 2.

(16) (a) Gredan, J. E. *J. Mater. Chem.* **2001**, *11*, 37. (b) Ramirez, A. P. *MRS Bull.* **2005**, *30*, 447. (c) Hopkinson, J.; Coleman, P. *Phys. Rev. Lett.* **2002**, *89*, 267201. (d) Anderson, P. W. *Science* **1987**, *235*, 1196.

(17) Hatnean, J. A.; Raturi, R.; Lefebvre, J.; Leznoff, D. B.; Lawes, G.; Johnson, S. A. *J. Am. Chem. Soc.* **2006**, *128*, 14992.

(18) (a) Cannon, R. D.; White, R. P. *Prog. Inorg. Chem.* **1988**, *36*, 195. (b) McCusker, J. K.; Jang, H. G.; Wang, S.; Christou, G.; Hendrickson, D. N. *Inorg. Chem.* **1992**, *31*, 1874.

(19) Duisenberg, A. J. M. *J. Appl. Crystallogr.* **1992**, *25*, 92.

(20) Duisenberg, A. J. M.; Kroon-Batenburg, L. M. J.; Schreurs, A. M. *J. Appl. Crystallogr.* **2003**, *36*, 220.

(21) SADABS, V2.05; Bruker AXS Inc.: Madison, WI.

(22) Sheldrick, G. M. *SHELXTL NT/2000*, Version 6.10; Bruker AXS Inc.: Madison, WI, 2000.

positions and were refined as riding atoms. All nonhydrogen atoms were refined with anisotropic thermal displacement parameters. Additional data collection and refinement details are given in Table 1. When the structure was solved and fully refined, the possibility of position interchange between manganese and sodium sites was explored, since the interexchange has been shown to be significant in some structures.^{23–27} This was done by refining each position as composed of Na and Mn, with partial occupations as parameters adding up to 1. The results showed that interexchange in the studied compound is not significant, and therefore all the discussion is based on the non-exchanged refinement.

Magnetic Susceptibility. The ZFC and FC magnetic susceptibility measurements at variable temperature, in the 2.2–298 K range, were performed on an assembly of small crystals firmly wrapped with Teflon tape in a gel capsule using a Cryogenics SX600 SQUID magnetometer at 0.02, 0.1, 1.0, and 50 kOe. The magnetization curves were recorded at 1.8 and 5 K, at fields ranging from 0 to 60 kOe. Diamagnetic corrections (estimated from Pascal constants) and sample holder contributions were taken into account. AC susceptibility, at various frequencies, was obtained as a function of temperature on a Quantum Design PPMS system with an AC excitation field of 10 Oe.

Results and Discussion

Synthesis. The solvothermal synthesis of the title compound was performed using $\text{Mn}(\text{CH}_3\text{COO})_2 \cdot 4\text{H}_2\text{O}$ and L-serine in a 2:1 molar ratio. It is important to note that if the reaction is carried out in the absence of serine $\text{Na}_3[\text{Mn}_3(\text{HCOO})_9]$ is not obtained. Since no source of formate was included in the initial reaction mixture, the presence of this anion in the final product may be ascribed to the decomposition of serine. Furthermore, the isolation of the Δ conformer as the only product could be due to the initial coordination of the manganese(II) ion with the chiral L-serine ligand, thus inducing the preferential spatial arrangement of the final formate species. Therefore, the decomposition reaction of the coordinated amino acid generates the formate species presenting the *syn-anti* coordination mode leading to the isolation of $\text{Na}_3[\text{Mn}_3(\text{HCOO})_9]$.

Yokoyama et al.²⁸ reported that if amino acids are heated in organic solvents such as DMF or DMSO under alkaline conditions, racemization or decomposition occurs. The decomposition in polar organic solvents is especially relevant to amino acids with reactive side chains, such as serine. On the other hand the rate of hydrolysis of DMF to formate and dimethylamine increases especially at basic conditions and high temperature.²⁹ Furthermore, Wang et al. have published that M(II) ions behave as catalysts for the hydrolysis of DMF, having isolated and structurally characterized

Table 1. Crystal Data and Structure Refinement for 1

empirical formula	$\text{C}_3\text{H}_3\text{MnNaO}_6$
FW/uma	212.98
crystal system	cubic
space group	$P2_13$
temperature (K)	293 (2)
wavelength (Å)	0.71073
a (Å)	9.2762(11)
V (Å ³)	798.2(2)
Z	4
δ (gr.cm ⁻³)	1.772
μ (mm ⁻¹)	1.687
$F(000)$	420
θ range (deg)	0.978 to 27.47
hkl range	$-4 \leq h \leq 11$ $-12 \leq k \leq 10$ $-12 \leq l \leq 9$
$N_{\text{tot}}, N_{\text{uniq}}$	2714, 581
$(R_{\text{int}}), N_{\text{obs}}$	(0.0138), 568
refinement parameters	
GOF on F^2	1.141
R1, wR2 (obs)	0.0248, 0.0741
R1, wR2 (all)	0.0265, 0.0719
max. and min $\Delta\rho$	0.479, -0.261

$[\text{Mn}(\text{HCOO})_3(\text{NH}_2(\text{CH}_3)_2)]$.³⁰ Since the isolated compound reported in this work is a pure phase of $\text{Na}_3[\text{Mn}_3(\text{HCOO})_9]$ we conclude that the coordination of serine to Mn(II) ions precludes the hydrolysis of DMF.

Structural Description. The compound crystallizes in the chiral cubic space group $P2_13$. The chirality arises from the fact that only one $\text{M}(\text{HCOO})_6$ enantiomer is present.³¹ According to the rules to identify optical isomers of octahedral complexes, the manganese environment is well described as having a Δ conformation. Other formate salts crystallizing in a chiral space group have been previously reported for $(\text{NH}_4)[\text{M}(\text{OOCH})_3]$, with $\text{M} = \text{Ni}, \text{Co}, \text{and Mn}$.¹⁴

The structure displays triangular Mn_3 building blocks, in which the metal centers are bonded through formate ligands in a *syn-anti* mode (Mn–Mn 5.697(1) Å). The structure also presents sodium ions as charge compensating cations. These two different metallic sites, one occupied by manganese(II) cations and the other by sodium ions are in an octahedral environment, as shown in Figure 1. The manganese(II) ion occupies an a site over the crystallographic 3^+ axis, and the same is true for the sodium ion, placed in a b site. The octahedral environment of manganese(II) is formed by six oxygen atoms, where two types of formate ligands are present (three of them bonded through O1 oxygen atoms and the other three through O2 oxygen atoms). All O–Mn–O angles are close to 90° or 180°. Each manganese(II) center has three sodium ions as neighbors, at a distance of 3.4350(6) Å. Selected bond distances and angles are listed in Table 2. Three manganese sites surround a sodium ion, defining an equilateral triangle. As imposed by the 3^+ axis, each manganese(II) ion is the common vertex of three of these triangles, as shown in Figure 2; although sharing one vertex, they are not coplanar. The lattice resulting from this arrangement has also six regular pentagons (see Supporting Information, Figure 1S)

(23) Leyva, A. G.; Polla, G.; Vega, D.; Baggio, R.; de Perazzo, P. K.; de Benyacar, M. A. R.; Garland, M. T. *J. Solid State Chem.* **2001**, *157*, 23.

(24) Baggio, R.; Stoilovab, D.; Garland, M. T. *J. Mol. Struct.* **2003**, *659*, 35.

(25) Baggio, R.; Stoilovab, D.; Polla, G.; Leyva, G.; Garland, M. T. *J. Mol. Struct.* **2004**, *697*, 173.

(26) Stoilova, D.; Baggio, R.; Garland, M. T.; Marinova, D. *Vib. Spectrosc.* **2007**, *43*, 387.

(27) Stoilova, D.; Baggio, R.; Garland, M. T.; Marinova, D. *J. Mol. Struct.* **2007**, *842*, 67.

(28) Yokoyama, Y.; Hikawa, H.; Murakami, Y. *J. Chem. Soc., Perkin Trans. 1*, 2001, 1431.

(29) Juillard, J. *Pure Appl. Chem.* **1977**, *49*, 855.

(30) Wang, X. Y.; Zhang, S. W.; Gao, S. *Inorg. Chem.* **2004**, *43*, 4615.

(31) Zhang, B.; Wang, Z.; Kurmoo, M.; Gao, S.; Inoue, K.; Kobayashi, H. *Adv. Funct. Mater.* **2007**, *17*, 577.

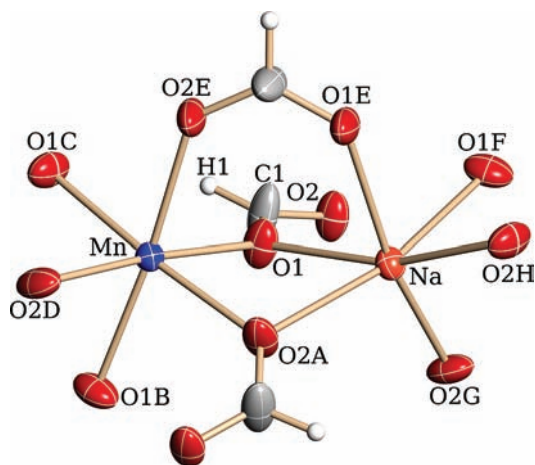


Figure 1. Molecular structure diagram for **1**, showing the asymmetric unit of the compound, and the symmetry equivalents that complete the octahedral environment for manganese(II) and sodium ions. The μ_2 -O, O' and μ_2 -O formate bridges connecting both metal centers are shown. Displacement ellipsoids are at the 50% level of probability. Labels are as follows: *a*: $1/2 + x, 3/2 - y, 1 - z$; *b*: $1/2 + z, 3/2 - x, 1 - y$; *c*: $3/2 - y, 1 - z, -1/2 + x$; *d*: $3/2 - z, 1 - x, -1/2 + y$; *e*: y, z, x ; *f*: z, x, y ; *g*: $1 - z, 1/2 + x, 3/2 - y$; *h*: $3/2 - y, 1 - z, 1/2 + x$.

Table 2. Selected Bond Distances (Å) and Angles (deg) for **1**^a

Mn–O1	2.207(2)	O1 Mn O1b	94.02(8)
Mn–O2a	2.207(2)	O2a Mn O2d	96.34(9)
Na–O1b	2.394(2)	O2a Mn O1c	175.09(8)
Na–O2a	2.381(2)	O2a Mn O1	81.48(8)
Mn...Na	3.4350(6)	O2c Mn O1b	88.29(9)
Mn...Mna	5.697(1)	Mn O1 Na	96.52(8)

^a *a*: $1/2 + x, 3/2 - y, 1 - z$; *b*: $1/2 + z, 3/2 - x, 1 - y$; *c*: $3/2 - y, 1 - z, -1/2 + x$; *d*: $3/2 - z, 1 - x, -1/2 + y$.

corresponding to a $3^3 \cdot 5^6$ topology.³² Differing from $(\text{NH}_4)[\text{M}(\text{OOCH})_3]$, the lattice shows no channels where the charge balancing ions are free to move, since the sodium ions are well confined in the structure. The cavity where the sodium ion is placed can be well described as a sphere with a diameter of 4.8 Å (two times the Na–O distance approximately), smaller than the 6.2 Å channel diameter described in $(\text{NH}_4)[\text{M}(\text{OOCH})_3]$.¹⁴ The way both metal ions, manganese(II) and sodium, are connected in $\text{Na}_3[\text{Mn}_3(\text{HCOO})_9]$ is different from what was observed for catena-(dodecakis(μ_3 -formato-*O,O,O'*)-hexa-manganese solvates,³³ or in the bimetallic sodium triformato-cadmium,³⁴ where one of the formate ligands connects the nearest metal centers in a μ_2 -O, O' fashion, while the other does so in a μ_2 -O mode. Moreover, this mixed bridging mode seems to be the main kind of bonding for bimetallic formates.

Magnetic Properties. ZFC and FC molar magnetic susceptibilities of $\text{Na}_3[\text{Mn}_3(\text{HCOO})_9]$ (**1**) were measured at different temperatures at 0.02, 0.1, 1.0, and 50 kOe (Figure 3 and Supporting Information, Figure 2S). Figure 3 shows the $\chi_M T$ versus *T* dependence obtained at 50 and 0.02 kOe. Magnetization irreversibility is observed below 40 K when the magnetic field is smaller than

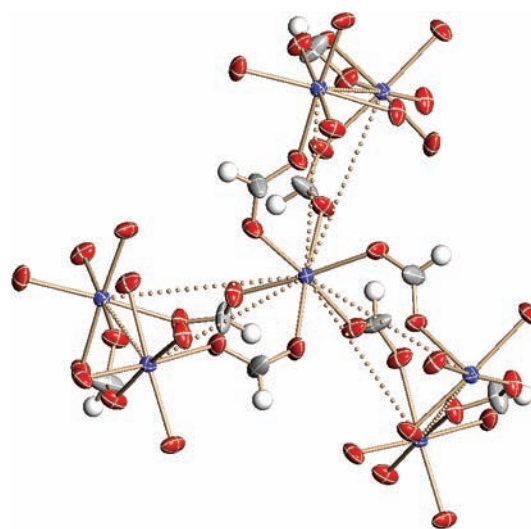


Figure 2. Lattice around Mn(II) ions. Sodium ions were omitted for clarity.

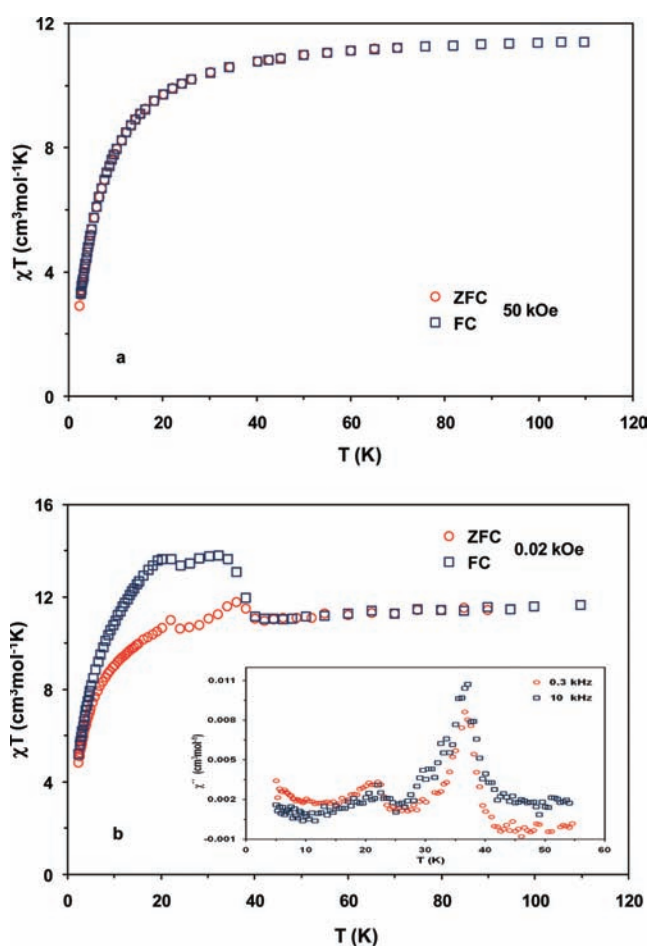


Figure 3. $\chi_M T$ vs *T* plots at (a) 50 kOe and (b) 0.02 kOe. Inset shows the temperature dependence of the AC susceptibilities of **1**, out-of-phase at frequencies of 0.3 and 10 kHz, with an AC excitation field of 10 Oe.

(32) Batten, S. R.; Robson, R. *Angew. Chem., Int. Ed.* **1998**, *37*, 1461.

(33) Wang, Z.; Zhang, B.; Kurmoo, M.; Green, M. A.; Fujiwara, H.; Otsuka, T.; Kobayashi, H. *Inorg. Chem.* **2005**, *44*, 1230.

(34) (a) Feliksinski, T.; Grochulski, P.; Kolasinski, W.; Wawrzak, Z. *Mater. Res. Bull.* **1982**, *17*, 627. (b) Antsyshkina, A. S.; Porai-Koshits, M. A.; Ostrikova, V. N. *Koord. Khim.* **1983**, *9*, 418.

1.0 kOe. Above 1.0 kOe, the ZFC and FC measurements are identical, showing a typical curve for a system with antiferromagnetic interactions between the Mn(II) centers. The value of $\chi_M T$ at 292 K is $12 \text{ cm}^3 \text{ mol}^{-1} \text{ K}$, which is slightly less than the value expected for three

uncoupled Mn(II) centers ($13.1 \text{ cm}^3 \text{ mol}^{-1} \text{ K}$) considering $g = 2.0$. The $\chi_M T$ value decreases smoothly from 292 to 40 K ($11 \text{ cm}^3 \text{ mol}^{-1} \text{ K}$); below this temperature the $\chi_M T$ values decrease faster to reach a value of $4.7 \text{ cm}^3 \text{ mol}^{-1} \text{ K}$ for 1.0 kOe at 2.2 K. It is important to point out that $\chi_M T$ at this temperature is different from the expected value for a system with $S = 5/2$ ($4.37 \text{ cm}^3 \text{ mol}^{-1} \text{ K}$, with $g = 2.0$), corresponding to one uncompensated Mn(II) ion. The magnetic susceptibility data obtained at 0.1 kOe (Supporting Information, Figure 2S) and 0.02 kOe (Figure 3) between 298 and 40 K show similar behavior to that described at higher fields. However, at low temperature the behavior observed is completely different, the $\chi_M T$ data rise giving maxima at 34 and 22 K, with $\chi_M T$ ranging from 12 (at 0.1 kOe) to $13 \text{ cm}^3 \text{ mol}^{-1} \text{ K}$, (at 0.02 kOe) for the FC measurements, and a lower value for the ZFC measurements. Below 22 K the value of $\chi_M T$ decreases rapidly to reach a value near $4.7 \text{ cm}^3 \text{ mol}^{-1} \text{ K}$ at 2.3 K. The significant irreversibility between ZFC and FC measurements observed at low field is still barely observed at 1.0 kOe. The sharp increase at low fields is typical of the appearance of a weak ferromagnetic moment because of spin canting away from a non-collinear antiferromagnetic alignment of neighboring spins.²

The in-phase AC susceptibility data χ' show only one small and frequency independent maximum at 37 K (Supporting Information, Figure 3S). The out-of-phase susceptibility data χ'' display two peaks at 37 and 21.5 K, corresponding to those observed in ZFC/FC DC susceptibility at low applied fields (inset Figure 3). The out-of-phase susceptibility is very small and close to the resolution limit of the susceptometer and does not show clear frequency dependence. Magnetization measurements at 1.8 and 5 K, as a function of field up to 60 kOe, show no hysteresis (Supporting Information, Figure 4S). It can be seen that at 1.8 K the value obtained for the magnetization at 60 kOe is close to $13 \mu_B$, which is still far from the expected saturation for three Mn(II) uncoupled ions ($15 \mu_B$). The $3^3 \cdot 5^6$ topology present in the $\text{Na}_3[\text{Mn}_3(\text{HCOO})_9]$ lattice contains two different kinds of polygons: triangles and pentagons formed by Mn(II) ions. Both polygons have odd numbers of vertices, and any antiferromagnetic spin coupling between the Mn(II) ions is expected to lead to spin frustration. The triangles can be considered as the building units of a 3D polymer with a complicated network, as shown in Supporting Information, Figure 5S. Five triangles sharing corners are connected to form pentagons, which are non-planar. Each Mn(II) is surrounded by six other Mn(II) ions, which are part of three triangles and six pentagons. As far as we know, there is no example in the literature of magnetic models of interacting spins in a similar lattice, with frustration and spin canting, which should be a theoretical challenge. We thus limit our interpretation using the simplest model for the studied system.

Using the isotropic Heisenberg–Dirac–Van Vleck Hamiltonian for an equilateral triangle, with nearest-neighbor exchange coupling J , $H = -J[\hat{S}_1\hat{S}_2 + \hat{S}_2\hat{S}_3 + \hat{S}_3\hat{S}_1]$,

where $\hat{S}_1 = \hat{S}_2 = \hat{S}_3 = 5/2$; χ_M is given by eq 1,³⁵ where $x = \exp(J/kT)$.

$$\chi_M = \frac{N\beta^2 g^2}{4kT} \left[\frac{340 + 455x^{15} + 429x^{28} + 330x^{39} + 210x^{48} + 105x^{55} + 20x^{60} + x^{63}}{4 + 7x^{15} + 9x^{28} + 10x^{39} + 10x^{48} + 9x^{55} + 4x^{60} + x^{63}} \right] \quad (1)$$

The best fit parameters obtained from eq 1 for the experimental data obtained in the range 40–300 K at 1.0 kOe, are $g = 1.91$, $J = -0.23 \text{ cm}^{-1}$ (Supporting Information, Figure 6S). The very small J value obtained is in agreement with the expected interaction for metal centers bridged by carboxylate ligands in a *syn-anti* coordination mode.³⁶ Besides, the observed magnetic behavior may be influenced by competing antiferromagnetic correlations between manganese triangles.

It is also possible to estimate the J value from the measured data using the mean field theory of antiferromagnetism, using $J/k_B = 3\theta/[zS(S+1)]$, where θ is the Curie–Weiss temperature, k_B is the Boltzmann constant, and z is the magnetic coordination number of the lattice site. The plot of χ_M^{-1} versus T for low field measurements obeys the Curie–Weiss law in the 40–300 K range with a Curie constant of $12.0 \text{ cm}^3 \text{ K mol}^{-1}$, and a negative Weiss constant θ of -5.7 K . The estimated value of the coupling constant J , with $S = 5/2$ and $z = 6$, is -0.22 cm^{-1} , which is similar to that the estimated from eq 1.

Finally, the experimental magnetic behavior of **1** can be summarized by the following observations: (i) antiferromagnetic interactions between the Mn(II) centers are evident, (ii) hysteresis for ZFC and FC measurements is observed for low applied field, (iii) two maxima are observed at 22 and 34 K for low applied fields, and (iv) no saturation in the magnetization is found at the lowest temperature and 60 kOe. These experimental facts may be indicative of canted antiferromagnetism.

Because of the existence of noncentrosymmetric *syn-anti* HCOO bridges linking the metal sites satisfying the requirement for the antisymmetric interaction, as in other metal formate frameworks,^{37,38} the spins can adopt non-collinear spin configurations, a canted antiferromagnetic structure which is hindered by the existence of the frustrated triangular structures in the lattice. The increase of the susceptibility at low fields and at 34 K can be associated with weak ferromagnetism. In fact, we found in this region small hysteresis magnetization behavior (see Supporting Information, Figure 7S) typical of weak ferromagnetic behavior appearing at 34 K and disappearing below 22 K. Therefore, we can only speculate that below 22 K longer range correlations between the spins end up averaging out the weak ferromagnetic moment, showing the general antiferromagnetic behavior. Further

(36) (a) Dey, S. K.; Bag, B.; Abdul Malik, K. M.; Salah El Fallah, M.; Ribas, J.; Mitra, S. *Inorg. Chem.* **2003**, *42*, 4029. (b) Zhao, W.; Song, Y.; Okamura, T.; Fan, J.; Sun, W.; Ueyama, N. *Inorg. Chem.* **2005**, *44*, 3330.

(37) Wang, Z.; Zhang, X.; Batten, S. R.; Kurmoo, M.; Gao, S. *Inorg. Chem.* **2007**, *46*, 8439.

(38) Sharma, C. V. K.; Chusuei, C. C.; Clérac, R.; Möller, T.; Dunbar, K. R.; Clearfield, A. *Inorg. Chem.* **2003**, *42*, 8300.

(35) Carlin, R. L. *Magnetochemistry*; Springer-Verlag: Berlin, 1986; p 275.

studies on single crystals should be done and other techniques such as neutron diffraction should be used to unravel this unusual behavior.

Conclusions

$\text{Na}_3[\text{Mn}_3(\text{HCOO})_9]$ is a new chiral 3D trinuclear Mn(II) formate exhibiting a triangular arrangement, which was obtained by solvothermal synthesis. This compound is one of the rare examples where it is possible to find the phenomena of chirality and spin frustration.

Through magnetic susceptibility measurements it was found that $\text{Na}_3[\text{Mn}_3(\text{HCOO})_9]$ presents a general antiferromagnetic behavior with a field dependent moment, presumably because of canting. At applied fields higher than 1.0 kOe the antiferromagnetic behavior appears as the main interaction, with a J value of the order of -0.2 cm^{-1} , as expected for metal centers bridged by carboxylate ligands in a *syn-anti* coordination mode. At applied fields lower than 1.0 kOe magnetic maxima at 34 and 22 K are observed. These phenomena can be attributed to the appearance and disappearance of a weak magnetic moment. The interesting but complicated network of

magnetic interactions with spin frustration, chirality, and antisymmetric exchange interaction requires further experimental and theoretical studies to explain the observed magnetic behavior.

Acknowledgment. The authors acknowledge financial support from FONDAP 11980002 project LDRX-UFF and CNPq, CAPES and FAPERJ.

Supporting Information Available: A scheme showing the pentagons formed with the triangular building blocks (Figure 1S); $\chi_M T$ vs T plots at 1.0 and 0.1 kOe (Figure 2S); temperature dependence of AC susceptibilities in-phase at frequencies of 0.3 and 10 kHz with an AC excitation field of 10 Oe (Figure 3S); field dependence of magnetization at 1.8 and 5K (Figure 4S); the equilateral triangle as a building block of the 3D $\text{Na}_3[\text{Mn}_3(\text{HCOO})_9]$ network. Blue spheres: considered as the origin; yellow spheres: first neighbors; red spheres: second neighbors and green spheres: third neighbors (Figure 5S); fit of the experimental data at 1 kOe (Figure 6S); field dependence of magnetization at 2.5, 23, 33, and 40 K (Figure 7S); the CIF file of $\text{Na}_3[\text{Mn}_3(\text{HCOO})_9]$. This material is available free of charge via the Internet at <http://pubs.acs.org>.